

## A New Correlation for Calculating Pseudo Skin Factor Due to Restricted-Entry

*Ramadan Emara*

*Mining and Petroleum Engineering Department, Faculty of Engineering, Al-Azhar University, Nasr City, Cairo, Egypt*

Received July 28, 2023; Accepted November 13, 2023

---

### **Abstract**

Partial completion processes of wells have been utilized by petroleum engineers for many years to prevent gas and/or water from coning in production wells. However, this technique results in an extra pressure drop, known as pseudoskin, which has an effect on well productivity. A detailed assessment of this extra pressure drop is critical to fully recognizing the presence of formation damage in pay zones that are producing with partial penetration. This investigation's objective is to present a simple empirical correlation that could be utilized in forecasting the skin factor due to limited entry. In this study, we investigated the presented model and the available models for assessing pseudoskin factors that were presented in the literature. Computer programs were developed to implement the chosen literature models. Subsequently, with an emphasis on producing wells, a sensitivity analysis was performed. The effects of formation thickness, vertical and horizontal permeabilities, borehole size, and the length of the perforating interval, as well as the elevation from the centre of the perforating interval to the end of the formation, were studied. It is proven that regardless of where the open interval is located, the presented equation shows adequately accurate estimations of the pseudo skin factor.

**Keywords:** *Pseudoskin factor; Near-wellbore region; Completion efficiency; Partial completion.*

---

## **1. Introduction**

Well penetration is the joint distance between the borehole and the production zones of the reservoir. In several situations, the perforations of a borehole do not match the reservoir's full thickness. Such cases are described as partial penetration or restricted entry. In a restricted entry borehole, the flow path is compelled to converge perpendicularly in the direction of the perforations. Flow pattern distortion causes fluids to travel a longer distance. A situation of this type leads to an additional pressure drop added to the one caused by uniform radial flow in the case of a totally penetrating borehole. Generally, this further pressure drop caused by a restricted entry can be described by a measure referred to as the "pseudo skin." When the pseudo-radial flow starts, this pseudo skin is a time-independent variable [1]. Several authors have investigated the restricted entry problem and its effects on the pressure response and productivity loss. An infinite series is the analytical solution to this restricted entry problem. This solution necessitates the use of a computer programme and requires time to complete. The goal of this research is to use a commercial simulator (Eclipse) to obtain pseudo skin data and introduce a simple correlation of this factor to reduce calculation time. The next sections of this work address the dimensionless variables that analytical solutions are dependent on, the author's methodologies through a literature review, the method for getting pseudo skin factor data, using regression analysis to develop a simple correlation for the limited entry skin factor and sensitivity analysis using the developed correlation and five approaches chosen from the literature.

## **2. Definition of dimensionless variables**

The equations utilized in this study to compute the skin factor due to limited entry will be described in the following section. These equations are valid for single-phase fluid flow with

low compressibility and constant viscosity. The vertical permeability is assumed to be different from the horizontal permeability in all mathematical models. The top and bottom of the reservoir are assumed impermeable, and gravitational effects are ignored. The pseudoskin factor,  $S_p$ , is only dependent on the dimensionless variables  $b$ ,  $h_D$ , and  $h_{UD}$ , indicated in Fig. 1 based on the assumptions given above.

$$b = \frac{h_p}{h_t} \quad (1)$$

$$h_D = \frac{h_t}{r_w} \sqrt{\frac{k_h}{k_v}} \quad (2)$$

$$h_{UD} = \frac{h_U}{h_t} \quad (3)$$

where  $h_p$ ,  $h_t$ ,  $r_w$ ,  $k_v$ ,  $k_h$ , and  $h_u$  denote the perforating interval length, the thickness of the pay zone, wellbore radius, vertical permeability, horizontal permeability, and the distance between the pay zone's top and the perforation's top, respectively.

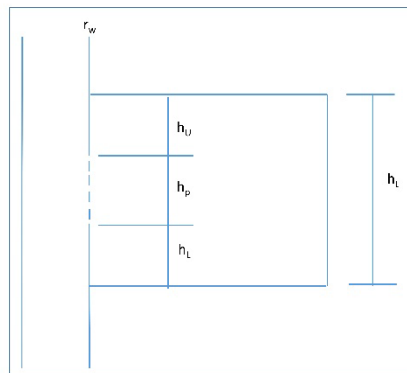


Fig. 1. Wellbore and formation geometrical parameters.

### 3. Literature review

Muskat investigated a steady-state model for an isotropic and homogeneous reservoir. The oil well was partially completed and the start of the perforation is adjacent to the top of the pay zone. For the inner boundary condition representation, Muskat considered the oil flow rate at the borehole to be uniform, i.e., in every part of the perforated distance, the oil flow rate is uniform. The solution he obtained is a function of the interval of the perforated depth. Muskat illustrated that the infinite conductivity in which the wellbore pressure stays fixed in every part of the completed interval is the most realistic inner boundary condition to model the borehole. However, the uniform flow model solution is easily obtained, while the infinite conductivity model solution can face many difficulties. Muskat introduced the term "equivalent point" at which the solutions of the uniform flow model and the infinite conductivity model are identical. He found that the equivalent point occurred at a perforated interval depth of 0.75. Muskat illustrated the deduction of an anisotropic solution from the isotropic case [2]. Brons and Marting presented a plot of the pseudoskin factor in response to the perforated ratio,  $b$ , and the thickness of the reservoir in relation to the size of the well,  $h/r_w$ , as a solution to the model of restricted entry in homogeneous and isotropic reservoirs [3]. Kazemi and Seth developed the Brons and Marting work for the anisotropic situation and the arbitrary location of the completed distance. They showed that the solution of an anisotropic case can be obtained from the solution plot of Brons and Marting if the term  $h_t/r_w$  is replaced by  $h_{UD}$  [4]. Odeh investigated the perforated interval generic position for steady-state flow considering a uniform flux wellbore model [5].

Odeh introduced a broad view of the solution of Muskat. The solution he presented is plots of productivity reduction in response to the geometrical parameters of the perforation. He introduced a mathematical equation that facilitates the calculation of the pseudoskin factor [6].

Gringarten and Ramey introduced a new approach to the computation of restricted entry problems based on the concept introduced by Muskat. They used the infinite conductivity model. In their approach, they divided the perforated interval into segments and assumed a uniform flux model in each segment. The pressure is constant at all the segments, and the gross flow rate is the aggregate of the flow rates from all the segments. Based on this methodology, the equation system ought to be solved every time for the flow rate in each segment and the pressure at the wellbore. Although their approach is reasonable, it needs a huge computational effort to attain the solution and includes complex implementation. They introduced a figure of the equivalent point versus  $h_D$  that was reliable for the situation of the perforation adjacent to the top of the reservoir or to the producing zone base. Based on this Fig., the infinite conductivity solution can be derived from the uniform flux solution [7].

Streltsova-Adams obtained the solution of the pseudoskin factor for a random location of the perforation using a uniform flux model. They considered two situations: first, the highest and the bottom of the reservoir are sealed; and second, the reservoir contains a gas cap. To remove the effect of pressure variation throughout the perforation, they integrated the uniform flow solution to calculate the average pressure at the borehole [8]. Papatzacos used an infinite conductivity wellbore model to derive the pseudoskin factor for a generic location of the perforated distance. The formula he presented does not include complex implementation [9]. Kuchuk and Kirwan investigated a uniform flux model for a partial perforation and introduced a pseudoskin factor formula. Also, they illustrated that the infinite conductivity solution is attained in accordance with the equivalent point plot, which was introduced by Gringarten and Ramey. The formula presented in their work is valid only when the start of the perforations begins at the top or bottom of the pay zone [10]. Yeh and Reynolds used a numerical reservoir simulator to study the effect of limited flow entry in a multilayer reservoir. For the single layer case, they introduced a pseudoskin factor formula for the arbitrary position of the perforated distance [11]. Vrbik investigated partial penetration problems using steady state flow and presented a pseudoskin factor formula. The presented correlation was derived for an incompressible system with consistent flow across the perforation [12-13].

In a single or multilayered reservoir with cross-flow between layers, Lee revealed how to determine the pseudo skin factor value for a well with only a section of the producing interval open to flow. A sealed reservoir's long-time pressure distribution is calculated using a pseudo-steady-state diffusivity equation, which was developed for this method [14]. Abobaker *et al.* [15] investigated partial penetration skin factor using numerical and experimental work. They used a radial flow cell (RFC), which was built by Ahammad *et al.* [16-17] to do twenty-five experimental runs. They injected water into a core sample and measured the pressure drop and single-phase flow rate. The water is radially injected within the Darcy flow in the core sample. Also, they used ANSYS DLUENT 18.1 for numerical runs. Table 1 lists the five models considered in this investigation from the literature.

Table 1. Summary of some studies' models of pseudo-skin factor.

Author(s)	Equations
(Streltsova-Adams, 1979)[8]	$S_p = \frac{2}{\pi^2 b^2} \sum_{n=1}^{\infty} \frac{1}{n^2} \{ \sin[n\pi(b + h_{UD})] - \sin(n\pi h_{UD}) \}^2 BesselK(0, \frac{n\pi}{h_D})$
(Kuchuk and Kirwan, 1987) [10]	$S_p = \frac{2}{\pi b} \sum_{n=1}^{\infty} \frac{1}{n} \sin(n\pi b) \cos(n\pi z_D^*) BesselK(0, \frac{n\pi}{h_D})$ $z_D^* = 0.9069 - 0.05499 \ln(bh_D) + 0.003745 [\ln(bh_D)]^2$
(Papatzacos, 1987) [9]	$S_p = \left( \frac{1-b}{b} \right) \ln \left( \frac{\pi h_D}{2} \right) + \frac{1}{b} \ln \left[ \frac{b}{b+2} \left( \frac{G-1}{H-1} \right)^{\frac{1}{2}} \right]$ $G = \frac{1}{h_{UD} + \frac{b}{4}} \text{ and } H = \frac{1}{h_{UD} + \frac{3b}{4}}$

Author(s)	Equations
(Yeh and Reynolds, 1989) [11]	$S_p = \left(\frac{1-b}{b}\right) [\ln(C'/b(1-b)h_D) - c_1]$ $c_1 = 0.481 + 1.01b - 0.838b^2$
(Odeh, 1980) [6]	$S_p = 1.35 \left\{ \left(\frac{1-b}{b}\right)^{0.825} [\ln(r_w h_D + 7) - [0.49 + 0.1 \ln(r_w h_D)] \ln(r_{wc}) - 1.95] \right\}$ $r_{wc} = r_w \exp[0.2126(z_{mD} + 2.753)]$ $z_{mD} = h_{uD} + \frac{b}{2}$

In the Yeh-Reynolds equation, the perforating interval position and the perforating ratio, *b*, determine the quantity *C'*. Once the perforating period occurs at the structure's top or bottom, *C'* = 2. We have *C'* = 1 when the formation's perforating interval occurs in the middle. In other cases, it is necessary to calculate the value of *C'* using a figure from Yeh and Reynolds [11]. An artificial neural network (ANN) model has been developed in this study to estimate the value of *C'*.

#### 4. ANN model development for C'

An ANN is a type of optimization tool that predicts an object's best performance given a set of input datasets. An ANN usually has one or more hidden layers, as well as an input and an output. Several processing elements are included in each layer (called neurons). By using connecting parameters (called weights), the neurons in each layer are connected to the neurons in the next layer [18-22].

The chart data was utilized to create a feed-forward neural network model with back-propagation training. 70% of the data was utilized in the training phase to reduce mean square error (MSE), while the remaining 30% was used to test and confirm the model's dependability and accuracy.

##### 4.1. Model architecture

The model consists of three layers: an input layer with one input, a hidden layer with five neurons that employs the Tan-sigmoid function as a transfer function, and an output layer with one estimated *C'* output. The architecture of the ANN model is shown in Table 2. Table 3 illustrates Input and hidden layer weights and biases, and biases and weights between the hidden and output layers.

Table 2. ANN model architecture and parameters.

Component	Value
Layers Count	3
The number of neurons in the input layer	1
The number of neurons in the hidden layer	5
Training algorithm	Levenberg-Marquardt
The hidden layer's activation function	Tan Sigmoid
The output layer's activation function	Pure-linear

##### 4.2. Mathematical model description

For *i* = 1 to no of neurons, the hidden inputs are calculated using the following expression:

$$S_{i,1} = \sum_{i=1}^5 (w_{i,1}x) + b_i \tag{4}$$

*x*: input, normalized of  $\frac{2\Delta z_D}{1-b}$ .

The normalized values can be obtained using the following expression:

$$x = 2*(x - X_{(min)})/(X_{(max)}-X_{(min)})-1 \tag{5}$$

The following formula can be used to compute *C'*:

$$C' = 0.5 * \left( \sum_{i=1}^5 w_{i,2} \left( \frac{2}{1+e^{-2S_{i,1}}} - 1 \right) + b_2 + 1 \right) + 1 \tag{6}$$

Table 3. Input and hidden layer weights and biases

Neuron #	w <sub>i,1</sub>	b <sub>i,1</sub>	W <sub>i,2</sub>	b <sub>2</sub>
1	1.893549	-15.3063	36.13444	-0.57307
2	0.043486	9.095388	-47.2234	
3	8.965245	11.82367	-78.9215	
4	-1.11017	-3.02243	35.06231	
5	64.97845	-137.169	-196.899	

### 5. Pseudoskin factor calculation approach

From the interpretation of well test, the total skin factor can be acquired by the following equation [23]:

$$s_t = s_p + \frac{S}{b} \tag{7}$$

where  $S_t$ ,  $S$ ,  $S_p$ , and  $b$  symbolize the total skin, mechanical skin, pseudoskin caused by restricted entry, and the proportion of perforated to total reservoir thickness, respectively.

The total skin factor, as determined by the preceding equation, is the sum of the effects of the pseudo skin factor and the real skin, as a result of damage or stimulation. The petroleum engineer can obtain the total skin from well test pressure data and also estimate the pseudo-skin factor using a correlation. Then real skin can be estimated to determine if the well needs stimulation or not. The dimensionless bottomhole pressure,  $P_{wD}$ , and dimensionless time,  $t_D$ , can be described by the following equation:

$$p_{wD} = \frac{k h (p_i - p_{wf})}{141.2 q \mu} \tag{8}$$

$$t_D = \frac{2.637 \cdot 10^{-4} k t}{\phi c_t \mu r_w^2} \tag{9}$$

If the pay zone is completely perforated, such that the length of the open interval,  $h_p$ , is equal to the total pay zone thickness,  $h_t$ , then a plot of dimensionless bottomhole pressure,  $p_{wD}$ , versus dimensionless time,  $t_D$ , on semilog coordinates shows a slope of 1.151 straight line, as displayed by the lowest line in Fig. 2.

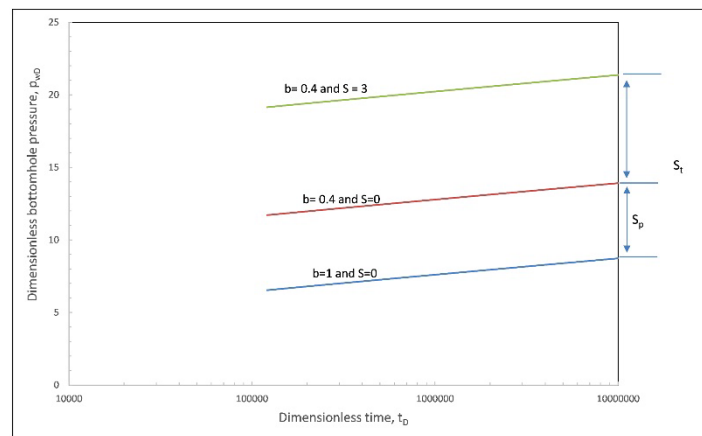


Fig. 2. Restricted entry well dimensionless pressure drop in a single layer reservoir.

For a partially perforating well, a plot of  $P_{wD}$  versus  $t_D$  still shows a slope of 1.151 straight line on semilog coordinates; see the middle line in Fig. 2. This semilog straight line was moved up from the one acquired in the whole perforation case by a fixed quantity for particular properties of the reservoir and the ratio of the interval of the perforation to the pay zone thickness,  $b$ . The complete penetration and partial penetration cases assume that the real skin factor is equal to zero; that is, no damage or stimulation. Supposing the model has been damaged close to the wellbore region, then the plot of  $P_{wD}$  versus  $t_D$  still shows a slope of 1.151 semilog

straight line on semilog coordinates as displayed by the highest line in Fig. 2. On the other hand, the amount by which this semilog straight line has moved up from the one that happens for the whole perforation represents the total skin factor,  $S_t$ . Then the pseudoskin factor represents the difference between the complete penetrating case and the restricted entry one.

### 6. Numerical simulation

Two cases are considered in this study; the first case is where the perforation interval starts from the pay zone's top. The perforation interval can be located anywhere between the crest and end of the pay zone in the second case. Table 4 illustrates the basic parameters inputted in the numerical simulator.

Table 4. Basic parameters inputted in the numerical model.

Parameter	Value	Parameter	Value
Wellbore radius, ft	0.333	Sand-face production rate, bbl/D	100
Reservoir Porosity	0.2	Initial pressure, psi	5000
Permeability in radial direction, mD	100	Oil viscosity, cp	5.9
Permeability in theta direction, mD	100	Rock compressibility, $\text{psi}^{-1}$	0.000004
Permeability in vertical direction, mD	36.07232	Oil formation volume factor, bbl/STB	1.1

#### 6.1. Open interval at top

We consider here the case where the open interval's top is adjacent to the formation's top boundary, as shown in Fig.3.

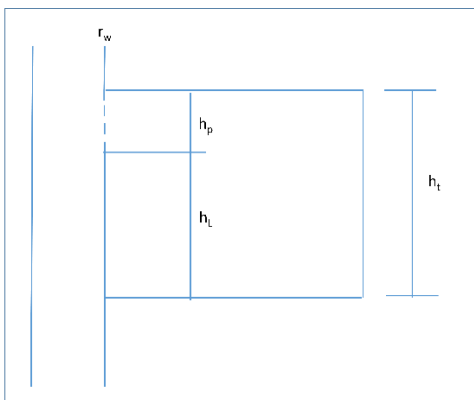


Fig. 3. Single layer reservoir.

Using a commercial reservoir simulator (Eclipse), an oil phase model with the following assumptions has been developed:

- Constant viscosity and small compressibility.
- The sand face flow rate is a constant at the wellbore.
- Well is positioned at the centre of a cylindrical
- The model is homogenous and has a uniform thickness.
- Horizontal permeability differs from vertical permeability.
- The pay zone's top and bottom are sealed.
- The start of the perforation is close to the top of the reservoir.

From all the analytical solutions in the literature, the pseudo skin factor is dependent on the total reservoir thickness, open interval length, well radius, horizontal permeability, and vertical permeability. These independent variables were grouped into two dimensionless numbers,  $b$  and  $h_D$ . To obtain the data to develop the pseudo skin factor correlation,  $b$  was assumed to take the values of 0.025, 0.05, 0.075, 0.1, 0.15, 0.2, 0.3, 0.4, 0.5, 0.6, 0.7, 0.8, 0.9, and 0.95, while  $h_D$  takes the values of 50, 100, 250, 500, 1000, 2500, 5000, 10000, 25000, and 50000. These ranges should encompass virtually all cases of practical interest.

##### 6.1.1. Example calculation

Two simulation runs were carried out to obtain a single value of skin factor due to limited entry. The first run in which the open interval length is equal to the total pay zone thickness (complete penetration). The second run, in which the open interval length is equal to 0.1 of the formation thickness (partial penetration,  $b=0.1$ ), therefore, the pseudo skin factor is the difference between the second run and the first one. The following Figure show this approach.

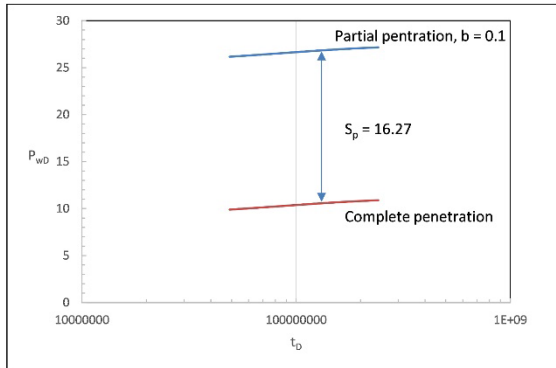


Fig. 4. Pseudo skin factor calculation.

$$S_p = m \ln(h_D) + c \tag{10} \text{ where}$$

$$m = \frac{0.937}{b} - 0.8274 \tag{10a} \text{ and}$$

$$c = \frac{0.001}{b^3} - \frac{0.0804}{b^2} - \frac{1.27}{b} + 1.4346 \tag{10b}$$

### 6.2. Arbitrary location of the open interval

In this case, we consider the single-layer case where the location of the open interval is arbitrary. The reservoir geometry for this case can be obtained from Fig.5 by setting the geometrical properties such as porosity, horizontal and vertical permeabilities to be the same for all layers [11]. This system allows us to move the open interval up and down along the reservoir.

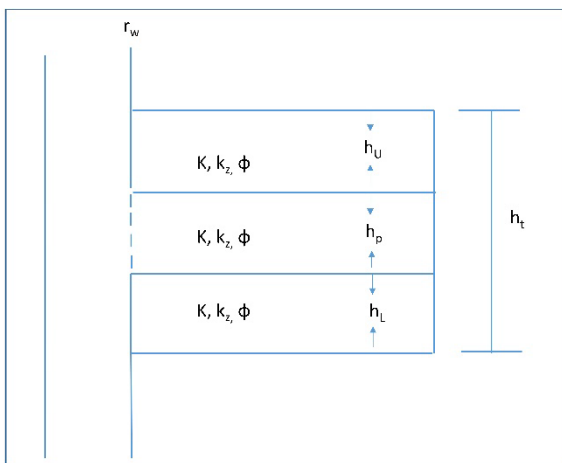


Fig. 5. Three layers reservoir.

This process is repeated for each value of  $b$  for all values of  $h_D$ , and then we used regression analysis to correlate the results to get a simple equation of pseudo skin factor. The concept of regression analysis is to minimise the error between the calculated pseudo skin factor from the equation and the measured one from the simulation. It has been noted that there is a linear relationship between pseudo skin factor,  $S_p$ , and  $h_D$  on a semilog scale. A number of 140 data sets collected from simulation runs were used to establish the following correlations.

When the perforating interval is next to the top of the perforation, the maximum pseudo skin factor occurs, and when the centre of the perforating interval corresponds with the centre of the formation, the minimum pseudo skin factor occurs. In this work, this comment was used to introduce a corrective graph to the developed pseudo skin factor correlation.

To investigate the influence of the open interval's arbitrary position on the value of the pseudo skin factor,  $b$  and  $h_D$  were considered to be the same as in the previous scenario. The distance between the reservoir's top and the perforation's top,  $h_U$ , (for example, when  $b = 0.1$ ), has values of 0.01,

0.03, 0.05, 0.1, 0.2, and 0.45. The pseudo skin factor is calculated in the same way as in the previous case. A total of 780 data sets have been collected from simulation runs to introduce the following correction graph (Fig. 6). As a result, the presented correlation has the following form:

$$S_p = m \ln(h_D) + c - \Delta S \tag{11}$$

where  $m$  and  $c$  do not change, and  $\Delta S$  can be obtained from the following Figure 6.

Fig. 6 assumes that,  $h_U = h_L$  and  $\Delta z = \frac{h_U}{h_t}$  to present our correlation for predicting  $\Delta S$ . When the top of the perforation is next to the formation's top,  $h_U = 0$ ,  $\Delta z = 0$ , and Fig. 6 shows that  $\Delta S = 0$ . Fig. 6 displays that for any perforation ratio, maximum  $\Delta S$  is achieved when the center of the open interval is next to the formation centerline, that is, when  $h_U = h_L$  and  $2\Delta z (1-b) = 1$ . When using Fig. 6 to estimate  $\Delta S$ ,  $\Delta z$  should be defined as  $\Delta z = \frac{h_L}{h_t}$  if  $h_U > h_L$ .

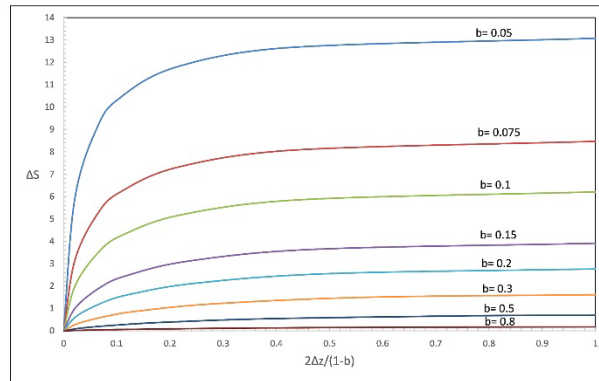


Fig. 6. Correlation for correction of pseudo-skin arbitrary location.

### 7. Results and discussion

A sensitivity analysis of the problem of estimating the skin factor due to limited entry for a vertical oil well is described in this section. A spider plot is utilized to accomplish this target. There are two main scenarios to examine, as shown in Table 5.

Table 5. Sensitivity analysis bas-cases.

Parameter	$h_t$ , ft	$h_p$ , ft	$k_v$ , mD	$k_h$ , mD	$r_w$ , ft	$h_u$ , ft
Base-case 1	40	5	60	120	0.3	0
Base-case 2	40	5	60	120	0.3	10

The perforated distance is poisoned near the crest of the pay zone in the first-case scenario. The perforated distance in the second-case scenario can be placed anywhere on the producing formation between the top and bottom. The mean of the pseudo skin factors generated from the presented correlation and the five chosen models is used to perform the sensitivity analysis for all correlated variables. The spider diagrams show how pseudo skin factors are affected by geometry-related parameters ( $h_t$ ,  $h_p$ ,  $r_w$ ) and reservoir attributes (horizontal and vertical permeabilities) (Figs. 7 and 8).

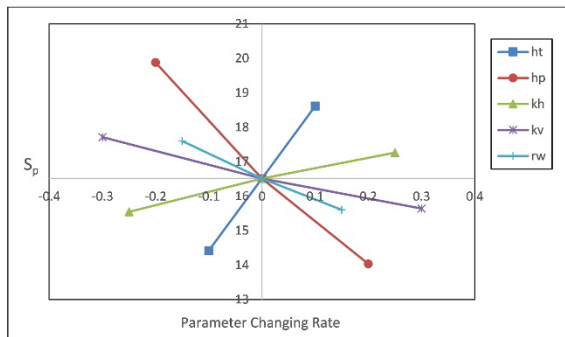


Fig. 7. Base-case 1 spider plot.

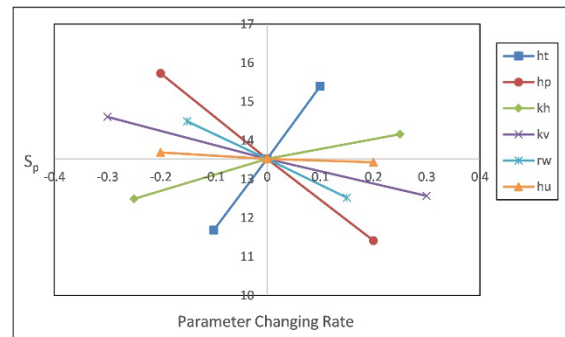


Fig. 8. Base-case 2 spider plot.

Tables 6 and 7 illustrate the sensitivity dependency gradients for all six methods. It is obvious that the presented correlation shows the same trend of dependency slopes for all correlated parameters as the five chosen models. The pseudo skin factor is clearly responsive to the thickness of the pay zone, followed by the length of the perforated interval on a secondary level.

Table 6. Pseudo-skin factor change rate- Base Case 1.

Parameter	Yeh-Reynolds	Odeh	Papatzacos	Streltsova	Kuchuk-Kirwan	This study
$h_t$	21.15	19.20	21.15	22.05	20.45	21.85
$h_p$	-14.45	-13.95	-14.48	-15.88	-13.45	-15.50
$r_w$	-6.87	-5.57	-7.03	-6.73	-7.33	-6.47
$k_h$	3.60	2.94	3.58	3.40	3.66	3.40
$k_v$	-3.62	-3.00	-3.53	-3.43	-3.73	-3.42

Table 7. Pseudo-skin factor change rate- Base Case 2.

Parameter	Yeh-Reynolds	Odeh	Papatzacos	Streltsova	Kuchuk-Kirwan	This study
$h_t$	16.50	19.25	17.45	17.45	—	17.70
$h_p$	-8.85	-13.65	-10.05	-8.70	—	-11.00
$r_w$	3.56	2.90	3.58	3.24	—	3.40
$k_h$	-3.62	-2.98	-3.62	-3.28	—	-3.45
$k_v$	-7.07	-5.60	-7.07	-6.40	—	-6.70
$h_u$	-0.58	-0.30	-0.52	-0.55	—	-0.60

### 7.1. Comparison of models

For each of the models previously mentioned, the pseudo-skin factor due to limited entry was computed. The following parameters were used to compare the pseudo skin: the perforated interval,  $h_p$ , the position of perforating interval,  $Z_{mD}$ , the formation thickness,  $h_t$ , the horizontal and vertical permeability,  $k_h$ , and,  $k_v$ , and the wellbore radius,  $r_w$ , (Figs. 9 to 14).

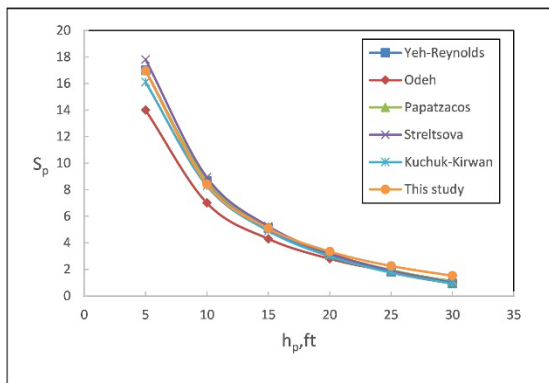


Fig.9. Pseudo-skin versus perforation interval (Base-case 1).

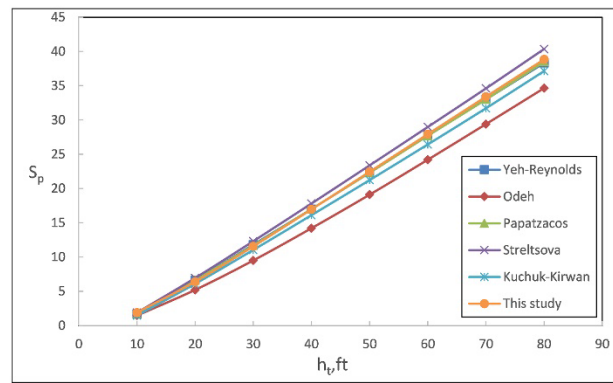


Fig.10. Pseudo-skin versus pay zone thickness (Base-case 1).

These graphs show a pattern that says, given the identical data input, the Streltsova formula yields a greater pseudo skin factor value, on the other hand, the Odeh method produces a lower pseudo skin factor value. Fig. 9 displays the responses of the six models to changes in  $h_p$ . The rate of change in Odeh's solution is the least. When  $h_p$  approaches the whole formation thickness,  $h_t$ , there will be no pseudoskin as expected. This indicates that the mechanical skin equals the total skin in this scenario and may be determined using typical well test procedures. Fig. 10 shows how the formation thickness has a significant impact on the pseudo-skin value. Due to the restricted flow, a great pay zone thickness with a small perforated interval will result in a great pressure decrease. This is similar to the movement of fluid via a small-diameter conduit. Two situations for  $Z_{mD}$  are evaluated, the borehole segment that has been prepped for production is placed at the crest of the pay zone, and a perforating interval can be placed anywhere between the crest and end of the producing formation.

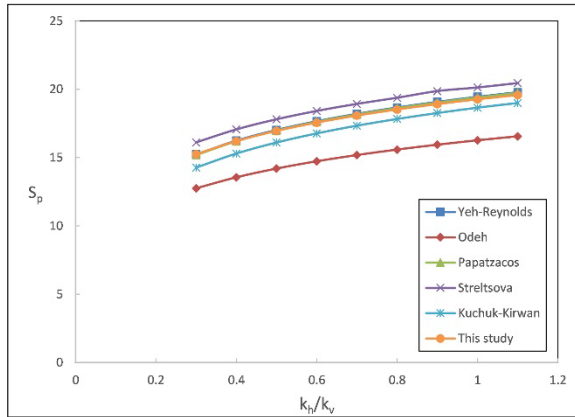


Fig. 11. Ratio of pseudo-skin to permeability (Base-case 1).

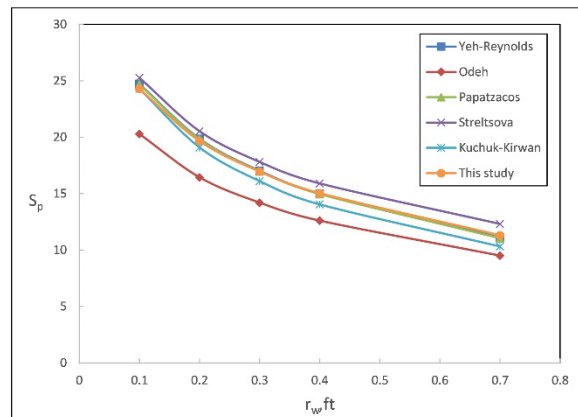


Fig. 12. Pseudo-skin versus wellbore radius (Base-case 1).

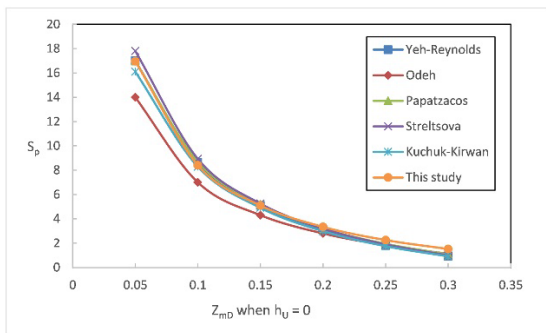


Fig. 13. Pseudo-skin versus  $Z_{mD}$  (Base-case 1).

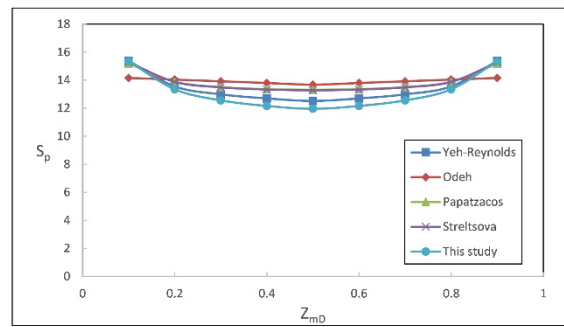


Fig. 14. Pseudo-skin versus  $Z_{mD}$  (Base-case 2).

Figs. 11 and 12 indicate that the pseudo skin factor value grows as the the ratio of anisotropy ( $k_h/k_v$ ) increases, while it reduces when the wellbore radius value increases. Fig. 13 represents the same trend as Fig. 9 for the first case.  $Z_{mD}$  is the function of  $h_p$  when  $h_u$  is fixed, therefore this is understandable. Once the perforating interval varies from crest to end, the presented correlation and the five models' pseudo skin result at a fixed amount. In the second situation, the variable for  $Z_{mD}$  is the perforating position. As shown from Fig. 14, the minimum value of the pseudo skin factor lies at  $Z_{mD} = 0.5$ . This is for the presented correlation and the models from the literature. This means that, the centre of the perforating interval coincides with the centre of the formation. As well as the value of the pseudo skin factor at the top of the formation equaling the value at the bottom of the formation. Except for Kuchuk and Kirwan, all of the models reveal the same trend for  $Z_{mD}$ .

### 8. Conclusions

This paper has highlighted the importance of the estimation of pseudoskin factor to answer the two practical questions: a) How much oil will be loss due to restricted-entry; and, b)

A straightforward method for generating pseudoskin factor data for a vertical oil well partially completed in a single layer reservoir was introduced. A simple correlation was proposed to estimate such pseudoskin factor. The correlation applies when the perforating interval placed in the pay zone between the top and bottom. The presented correlation covers a data wide range to encompass virtually all cases of practical interest and showed a good match in comparison to the literature correlations. A sensitivity analysis was carried out, as well as a model comparison. The total pay zone thickness affects the pseudoskin factor more than any

other variable, followed by the length of the perforating interval. The Streltsova formula produces the biggest pseudoskin factor values, whereas the Odeh formula produces the smallest pseudoskin factor values.

### Nomenclature

$b$	<i>Dimensionless variable, defined by Equation (1)</i>
$c_t$	<i>System compressibility; <math>\text{psi}^{-1}</math></i>
$h_L$	<i>Distance to the perforating interval from the bottom of the pay zone, ft</i>
$h_U$	<i>Distance to the perforating interval from the crest of the pay zone, ft</i>
$h_D$	<i>Dimensionless variable, defined by Equation (2)</i>
$h_p$	<i>Perforating interval thickness; ft</i>
$h_t$	<i>Pay zone thickness; ft</i>
$k$	<i>Absolute permeability; mD</i>
$k_h$	<i>Horizontal permeability; mD</i>
$k_v$	<i>Vertical permeability; mD</i>
$p_i$	<i>Initial pressure, psi</i>
$P_{wD}$	<i>Dimensionless variable, defined by equation (5)</i>
$p_{wf}$	<i>Wellbore flowing pressure, psi</i>
$q$	<i>Sand face flow rate, RB/D</i>
$r_w$	<i>Wellbore radius; ft</i>
$r_{wc}$	<i>Corrected wellbore radius, Odeh equation; ft</i>
$S$	<i>Mechanical skin (formation damage); dimensionless</i>
$S_p$	<i>Pseudoskin dimensionless variable</i>
$S_t$	<i>Total skin; dimensionless</i>
$t$	<i>Time, hours</i>
$t_D$	<i>Dimensionless variable, defined by equation (6)</i>
$Z_{mD}$	<i>Dimensionless variable, Odeh equation</i>
$\Phi$	<i>porosity; fraction</i>
$\mu$	<i>viscosity; cp</i>

### References

- [1] Streltsova TD. Well testing in heterogeneous formations. United States 1987.
- [2] Muskat M. The flow of homogeneous fluids through porous media. International Human Resource Development Corporation, Boston 1982.
- [3] Brons F, Marting V. The effect of restricted fluid entry on well productivity. Journal of Petroleum Technology 1961;13(02):172-4.
- [4] Kazemi H, Seth MS. Effect of anisotropy and stratification on pressure transient analysis of wells with restricted flow entry. Journal of Petroleum Technology 1969;21(05):639-47.
- [5] Odeh. Steady-state flow capacity of wells with limited entry to flow. Society of Petroleum Engineers Journal 1968;8(01):43-51.
- [6] Odeh. An equation for calculating skin factor due to restricted entry. Journal of Petroleum Technology 1980;32(06):964-5.
- [7] Gringarten AC, Ramey H. An approximate infinite conductivity solution for a partially penetrating line-source well. Society of Petroleum Engineers Journal 1975;15(02):140-8.
- [8] Streltsova-Adams T. Pressure drawdown in a well with limited flow entry. Journal of Petroleum Technology 1979;31(11):1469-76.
- [9] Papatzacos P. Approximate partial-penetration pseudoskin for infinite-conductivity wells. SPE Reservoir Engineering 1987;2(02):227-34.
- [10] Kuchuk FJ, Kirwan PA. New skin and wellbore storage type curves for partially penetrated wells. SPE Formation Evaluation 1987;2(04):546-54.
- [11] Yeh N, Reynolds A. Computation of the Pseudoskin factor caused by a restricted-entry well completed in a multilayer reservoir. SPE Formation Evaluation 1989;4(02):253-63.
- [12] Vrbik J. Calculating the pseudo-skin factor due to partial well completion. Journal of Canadian Petroleum Technology 1986;25(05).
- [13] Vrbik J. A simple approximation to the pseudoskin factor resulting from restricted entry. SPE formation evaluation 1991;6(04):444-6.
- [14] Lee K. A new method for computing pseudoskin factor for a partially-penetrating well. SPE Asia Pacific Oil and Gas Conference and Exhibition. OnePetro; 2001.

- [15] Abobaker E, Elsanouse A, Khan F, Rahman MA, Aborig A, Noah K. Quantifying the partial penetration skin factor for evaluating the completion efficiency of vertical oil wells. *Journal of Petroleum Exploration Production Technology* 2021;11(7):3031-43.
- [16] Ahammad M, Rahman M, Zheng L, Alam J, Butt S. Numerical investigation of two-phase fluid flow in a perforation tunnel. *Journal of Natural Gas Science Engineering* 2018;55:606-11.
- [17] Ahammad M, Rahman MA, Butt SD, Alam JM. An experimental development to characterise the Flow phenomena at THE Near-Wellbore Region. *International Conference on Offshore Mechanics and Arctic Engineering*. 58875. American Society of Mechanical Engineers; 2019:V008T11A19.
- [18] Gomaa S, Emara R, Mahmoud O, El-Hoshoudy A. New correlations to calculate vertical sweep efficiency in oil reservoirs using nonlinear multiple regression and artificial neural network. *Journal of King Saud University-Engineering Sciences* 2021.
- [19] Gomaa S, Soliman AA, Mohamed A, Emara R, Attia AM. New Correlation for Calculating Water Saturation Based on Permeability, Porosity, and Resistivity Index in Carbonate Reservoirs. *ACS Omega* 2022.
- [20] Gomaa S, Soliman AA, Nasr K, Emara R, El-hoshoudy A, Attia AM. Development of artificial neural network models to calculate the areal sweep efficiency for direct line, staggered line drive, five-spot, and nine-spot injection patterns. *Fuel* 2022;317:123564.
- [21] Gouda A, Gomaa S, Attia A, Emara R, Desouky S, El-hoshoudy A. Development of an artificial neural network model for predicting the dew point pressure of retrograde gas condensate. *Journal of Petroleum Science Engineering* 2022;208:109284.
- [22] El-Deen SAE, Farahat MS, Kamel S, Nouh AZJP, Coal. Drilling Vibration Modes and Penetration Rate Modeling using Artificial Neural Network and Multiple Linear Regression Analysis in Khoman Formation at the Egyptian Western Desert. *Petroleum & Coal* 2021; 63.(4).
- [23] Cunha L, Gui P, Zhang C. A Theoretical and Numerical Investigation of the Pseudoskin Factor. *Canadian International Petroleum Conference*. OnePetro; 2005.

---

*To whom correspondence should be addressed: Ramadan Emara, Mining and Petroleum Engineering Department, Faculty of Engineering, Al-Azhar University, Nasr City, Cairo, Egypt; e-mail: [ramadan.emara@azhar.edu.eg](mailto:ramadan.emara@azhar.edu.eg)*